Fracture 1977, Volume 1, ICF4, Waterloo, Canada, June 19 - 24, 1977

THE DESIGN AND FAILURE ANALYSIS OF A CARGO CONTAINMENT SYSTEM FOR A LIQUID NATURAL GAS SHIP

D. J. Burns*, R. J. Pick* and T. Brown**

ABSTRACT

Liquified natural gas is transported in ships at 111 K and near atmospheric pressure. In general a containment system has three components: a liquid tight shell designed to serve as the primary barrier separating the cargo from the ship hull, a secondary barrier designed to contain for a short time any leakage from the primary barrier, and an insulation system designed to keep cargo boil-off and inner hull temperatures at acceptable levels.

The forces imposed on a containment system are examined. Techniques used to assess the fatigue and fracture resistance of primary and secondary barriers are discussed. Where possible the discussion is illustrated by reference to the authors' practical experience of the design and evaluation of such systems.

1. INTRODUCTION

Cryogenic liquification will reduce 600 m^3 of natural gas to about 1 m^3 of liquid. At atmospheric pressure, liquified natural gas (LNG) has a boiling point of about 111 K and a specific gravity of about 0.45.

LNG is transported in ships with the liquid at slightly above atmospheric pressure. The low cargo density and requirement for separate water ballast containment leads to a relatively deep ship hull with low draft and high freeboard. Table 1 lists typical dimensions of some of the ships built to Conch specifications over the last fifteen years. It will be noticed that ships currently under construction have a cargo capacity five times that of the world's first commercial LNG tankers, Methane Princess and Methane Progress, which delivered their first cargoes in October, 1964 [1].

Various cargo containment systems have been developed or proposed to utilize the relatively deep ship hull [2]. The main requirements of any design of cargo containment system are to minimize loss of gas by heat ingress and to keep the steel structure of the ship at an acceptable temperature. In general a containment system has three components. A liquid tight shell designed to serve as the primary barrier separating the cargo from the ship hull. A secondary barrier designed to contain for a short time, e.g., fifteen days, any envisioned leakage of liquid cargo through the primary barrier. An insulation system designed to keep the cargo boil-off and inner hull temperature at acceptable levels. In some cases the secondary barrier is an integral part of the insulation system; in others it may only be a drip tray under the primary barrier with splash shields at the sides.

* Department of Mechanical Engineering, University of Waterloo, Waterloo, Ontario, Canada
** Conch LNG, Moorestown, New Jersey, U. S. A.

The structural complexity of the primary barrier and consequent reliability of any stress and failure analyses dictate the extent of the secondary barrier and the need for a failure analysis of the secondary barrier. This paper will review some of the factors considered in the design and failure analysis of primary and secondary barriers. Where possible the discussion is illustrated by reference to the authors' experience in the design and evaluation of the containment systems used for the ships listed in Table 1.

2. PRIMARY BARRIER CLASSIFICATIONS

All classification societies recognize three basic tank (primary barrier) designs [3]. Their general characteristics are:

2.1 Independent Tanks

These are sometimes called self-supporting or free-standing tanks. They have in themselves sufficient structural strength to withstand the loads imposed on them by the cargo and their interaction with the ship hull. They generally do not contribute to the structural strength of the ship. They can be further classified as gravity or pressure tanks. Gravity tanks are primarily prismatic in shape and loads are carried by bending stress. Pressure tanks are generally spherical or cylindrical in shape and loads are carried by membrane stress. Aluminum 5083-0 alloy and 9 percent nickel steels are the materials normally used for independent tanks.

2.2 Membrane Tanks

These are thin metallic linings which are supported completely by a load bearing insulation which in turn is supported by the ship's structure. A variant on these non-self-supporting gravity tanks is the semi-membrane design. In this design the metallic lining is not completely supported by the load-bearing insulation in that it is free of supports at the corners. Austenitic stainless steels (AISI 304 and 316) and a 36 percent nickel-iron-alloy (Invar) have been used for membrane tanks.

2.3 Integral Tanks

These are generally prismatic in shape and form an integral part of the hull. Therefore, they are subjected to the same loads as the adjacent hull structure. A number of companies are working on the so-called wet wall system. The LNG is contained by layers of foamed plastic on the inner hull. The foamed plastic acts as a tank and insulation. This technique has already been used for carrying liquid propane at 233 K.

Although all classification societies and regulatory bodies recognize these three basic classes of cargo tank, they often differ in their requirements for the fatigue and fracture analysis of a particular class of tank and its associated secondary barrier. A detailed review of these differences and the many factors which must be considered when designing LNG containment systems [1 - 3] is beyond the scope of this paper, but some general principles will be discussed.

3. FAILURE ANALYSIS OF THE PRIMARY BARRIER

3.1 Fatigue Analysis

The primary barrier design is dictated by the cargo and shiploads imposed on it during cargo unloading and loading and operation at sea. Of particular importance are the loads induced by the encountered waves. These loads usually vary in an irregular fashion with an average period of 5 - 10 seconds. These cyclic loads are dependent on ship heading, route and weather changes during voyages and from season to season.

If a fatigue analysis of the primary barrier is required the load spectrum used is usually the largest load spectrum the ship will experience during 10^8 wave encounters (20 years approximately) on the North Atlantic, Figure 1. The cumulative effect of this spectrum on fatigue of the primary barrier is then often obtained from the Miner-Palmgren rule where

$$\Sigma \frac{n_i}{N_i} < C_w$$

where, n_i is number of stress cycles at each stress level during the life of the ship; N_i is the number of cycles to failure for that stress level on the endurance (Wohler) curve, Figure 1; C_w is a coefficient determined by the classification society dependent on the test procedures and data used to generate the endurance curve.

An approach to this cumulative damage analysis, recommended by some classification societies, is to replace the load spectrum (load-frequency curve in Figure 1) by eight fatigue loads (i = 1 to 8). These alternating loads $\pm P_i$, are calculated from

$$P_i = \frac{17 - 2i}{16} P_o \qquad (1)$$

the number of cycles at that load is given by

$$n_i = 0.9 \times 10^i \qquad (2)$$

and the Miner-Palmgren rule is written as

$$0.9 \sum_{i=1}^{i=8} \left[\frac{10^i}{N_i}\right] + \frac{10^3}{N_9} < 0.5$$

where P_o is the load at a probability level of 10^{-8}; N_i is the number of cycles to failure for wave induced fatigue load $\pm P_i$; N_9 is also included as the number of cycles to failure for the fatigue load due to loading/unloading.

The basis of equations (1) and (2) is illustrated in Figure 1. Consider two load levels P_a and P_b. There will be n_a cycles of load exceeding P_a and n_b cycles exceeding P_b. Therefore there will be $n_a - n_b$ cycles of load at levels greater than P_a and less than P_b. For this example

$$n_i = n_a - n_b = 10^4 - 10^3 = 0.9 \times 10^i$$

and the effect of using equation (1) tends to give

$$P_1 = \frac{17 - 2i}{16} P_o \approx \frac{P_a + P_b}{2} .$$

3.2 Fatigue Analysis of Conch Ocean Membrane

The application of this approach to the Conch Ocean membrane tank has been described previously [4, 5]. Only a brief description will be given here. The membrane tank is an improved version of that used in the first membrane ship, Pythagore [2], combined with a modified version of the insulation/secondary barrier system used on the first commercial self-supporting tank ships, Methane Princess and Methane Progress [1]. Figure 2 shows a section of a right angle corner of this design.

A number of layers of balsa, glued together, form the core of the insulation. This core is faced with plywood to make insulation panels which are bonded to hardwood grounds, fixed to the double hull in a rectangular pattern. The spaces between the grounds are packed with mineral wool. Insulation continuity is ensured between the panels by means of expanded polyvinyl chloride wedges, compressed and bonded to the panels. These wedges are covered with plywood scabs. The plywood assembly is covered by a facing of balsa which is machined to give a smooth, flat surface onto which is fitted the membrane. The plywood assembly acts as a secondary barrier for the LNG if there should be a serious leak in the membrane.

The thin stainless-steel membrane is an assembly of corrugated sheets. The sheets, which are lap-welded together, have wave-shaped corrugations in two perpendicular directions. One wave is slightly smaller than the other and at their intersections they form a complex expansion joint known as a knot. Each set of corrugations is parallel to one of ship's axes and therefore to one of the tank axes. Along the edges of the tank (i.e., along the junction of any two walls) the corrugations on adjacent walls are joined by angle pieces with a corrugation which includes a special corner knot, Figure 2.

Along the edges of a tank the balsa facing pads are replaced by hardwood blocks glued onto the plywood facing of the insulation panels. Rigid stainless-steel angle pieces are bolted to these hardwood blocks. The edges of the membrane sheets are welded to these rigid angle-pieces so that when the tank is cooled the edge loads are transferred through the insulation to the ship structure.

When a tank is cooled, thermal stresses are induced in the membrane because of the restraint at the edges and the thermal gradient across the load-bearing insulation.

At sea the wave motion produces two types of cyclic mechanical stress in the tanks. Cargo motion produces a cyclic pressure spectrum which can be related to histograms showing the probability of occurrence of various sea states and the resulting bow accelerations of the ship [3]. These cyclic pressures which apply a combination of cyclic bending and pressure to the knots have the most serious effect on those knots near the edges of

the tank which straddle the junction between the stainless-steel angle and hardwood facing on the pads. Hull bending produces a cyclic elongation and contraction spectrum in the membrane which can be estimated by a method similar to that used for the pressure spectra [3].

Tests on components (knots) of the membrane were used to determine the general shape of the Wohler curve, Figure 1, and possible modes of failure. Then cyclic pressure tests on pilot size tanks were used to show the effects of construction irregularities and necessary tolerances on fatigue life.

Each pilot scale tank contained full-size components of membrane and insulation. Each tank contained 44 knots. It was necessary to terminate these tank tests before many of these knots had failed. Likelihood analysis was used to analyse this data [5] since conventional statistical techniques cannot handle such a severely truncated distribution. These likelihood estimates were then used to fix the position of the Wohler curve for a cumulative damage analysis similar to that described above.

3.3 Fracture Mechanics Analysis

The above safe-life analysis does not distinguish between fatigue crack initiation and propagation. In some cases separate studies are made of fatigue crack propagation from part-through thickness defects cut in critical areas of the primary barrier [6 - 8]. Such studies are used to demonstrate that small defects, missed by the construction quality control, will grow very slowly and will not reach a critical size before growing through the wall. A study of the subsequent growth of the through-thickness defect allows one to calculate leakage rates [9] and assess the time (size) margin between first detection of the leak and the crack becoming a critical size.

The reliability and extent of a fracture mechanics analysis of this type is one of the factors considered by the classification societies and regulatory bodies when specifying the extent of the liquid-tight secondary barrier for a particular type of tank. For example, the United States Coast Guard (USCG) recommendations for some types of independent tanks are:

1) Use analytical tools such as three-dimensional finite element or finite difference analysis and photoelastic analysis to determine the maximum stress field patterns, paying particular attention to support attachments and tolerance limits.

2) Subject the material to a fracture mechanics analysis in order to determine the critical crack size and the crack propagation rate with a given maximum stress, either at an assumed level or as computed above. Also determine the fracture mechanics properties (either from tables for well-documented materials or determined experimentally for lesser researched materials) for the material being used in the design.

3) Determine the minimum flaw size that will allow the passage of sufficient gas to be sensed by the gas detectors. Using the minimum flaw size that will allow the passage of sufficient gas to be sensed by the gas detectors, determine the length to which this crack will grow during the greatest of the following:

(a) two weeks,
(b) the time required to unload the cargo in an emergency, including the time to remove the cargo contained between the primary and secondary barriers,
(c) the anticipated average vessel running time between cargo loading and discharge points.

4) Compare the crack length after growth with the critical crack length. If the critical crack length is larger than the crack length after growth (designs approved to date have had ratios of approximately 10:1) then the design is acceptable.

Perhaps the best known application of this approach is the work of Det Norske Veritas [6] and Alcoa [9] on the spherical tanks of the Moss-Rosenberg design. These tanks consist of a spherical shell supported in the ship by a cylindrical skirt welded to an equatorial ring on the sphere. This ring is machined from thick 5083-0 plate. To demonstrate the leak before failure behaviour of these tanks Kelsey et al [9] fatigued surface flawed plates 1050 mm wide, 1500 mm long and 135 mm thick. A transverse groove cut on one side of two of these plates was used with longitudinal (axial) and side loading to simulate the actual loading in an equatorial ring. In one case a starter notch, 3 mm deep by 50 mm long was cut at the base of the transverse groove, where the plate thickness had been reduced to 83 mm. This starter notch was precracked to 22.1 mm deep by 63.9 mm long before applying a stress spectrum simulating six months of ship operation. This only increased the depth by 1 mm and the length by 2 mm. To grow the defect through the thickness if was necessary to apply cyclic loads far beyond those expected in service. At penetration the crack length on the groove (starting) side was 308 mm, i.e., about three times the plate thickness at the bottom of the groove.

After measuring leakage rates through this crack it was extended by fatigue to a length of 565.7 mm on the initiation side and 498.5 mm on the penetration side. It was then cooled to 203 K and fractured by static loading. This and other specimens failed by slow ductile tearing at net section fracture stress/yield stress ratios of 1.2 to 1.4. Since the fracture toughness of this material tends to increase with decrease in temperature this test gives a good indication of the fracture toughness available at service temperature.

Tenge et al [6] have used 5083.0 data, the Paris fatigue crack propagation equation and three dimensional finite element analysis to compute the growth of semi-elliptical surface cracks under the action of the expected sea spectrum. Figure 3 summarizes some of their calculations for periods exceeding the lifetime of a ship and Figure 4 illustrates for a 71 mm plate the crack length at penetration for varying ratios of bending ($\Delta\sigma_b$) to axial ($\Delta\sigma_a$) stress.

4. FAILURE ANALYSIS OF THE SECONDARY BARRIER

The classification of the primary barrier dictates the extent of the secondary barrier. The secondary barrier specification is dictated by the thermal and ship loads imposed on it during normal service operations and the requirement that it be capable of containing the cargo for a short period of time in the event of a significant leak from the primary barrier. The USCG requirements shown earlier indicate how the timescale for this "accident" can be set.

Since the secondary barrier is subjected to dynamic loads during normal operation it is usually necessary to assess its fatigue behaviour during the expected ship life and the effects of an accident at sometime during the ship life. As well as demonstrating that it can contain the cargo during the accident period it is desirably to demonstrate that the accident has no effect on the subsequent performance of the secondary barrier during normal operation.

The remainder of this paper will describe one design of independent tank and discuss some aspects of the evaluation of the fatigue performance of its secondary barrier. The 5083-0 aluminum alloy tank and the balsa/plywood/foam insulation and secondary barrier are evolved from the containment systems used for the Methane Princess and Methane Progress [1] and the insulation/secondary barrier of the Conch Ocean Membrane.

4.1 Free Standing Tank

Figure 5 shows the layout of an LNG ship and the general shape of the 5083-0 Al alloy, prismatic, free-standing tank which will be lifted into a hold already lined with the insulation and secondary barrier.

Figure 6 shows details of one of the cargo tanks. Each cargo tank is subdivided into two compartments by a liquid-tight longitudinal centerline bulkhead. In addition, each liquid-tight compartment is further subdivided by a transverse, non-liquid-tight, swash bulkhead. Thus, in plan form, the midships tanks are divided into four equal quadrants. The forward and aft tanks, which taper to follow the shape of the ship, Figure 5, are also divided into four quadrangles, but these are only symmetrical with respect to the longitudinal centerline of the tank. The position of the cargo tank in the insulated hold is maintained transversely by roll keys, fitted to the top and bottom of the tank in way of the longitudinal centerline buklhead, and longitudinally by fore and aft pitch keys fitted to the tank top in way of the transverse bulkhead. Additional restraint against tank movement relative to the ship is provided by the friction between the cargo tank bottom and the supporting balsa-plywood pads (island panels). These pads are located along the centerline bulkhead, the bottom longitudinal girders (of which there are as many as eight in the midships tanks) and the forward and aft bulkheads, Figures 6 and 7.

The primary load bearing structure in the tank consists of the deep horizontal ring frames and the top and bottom longitudinal girders. A transverse "ring-type" structure composed of the extruded stiffeners acting in conjunction with the shell plating provides the necessary load path to transfer the hydrostatic pressure loading existing on the shell plating to the principal structural elements (horizontal ring girders and longitudinal girders). At the end bulkheads, vertical extruded stiffeners are employed and act in the same manner as the transverse stiffeners do in transferring the hydrostatic loading.

As mentioned earlier, there have been numerous studies of the fatigue crack propagation and fracture behaviour of this material. The finite element techniques used to analyse this tank have been described previously [10]. The design for a particular element or region of the tank is established by considering a combination of loading conditions, in particular:

a) static cargo fluid pressure plus gas overpressure,
b) dynamic cargo fluid pressure plus gas overpressure,
c) overall longitudinal ship deformation corresponding to the worst expected hogging or sagging moment,
d) local deformation of the ship's bottom (longitudinal and transverse) occurring between cofferdams, i.e., over each cargo hold,
e) thermal gradients during cool-down, warm-up and ballast voyage,
f) flooding of the cargo hold producing an external pressure on the tank bottom,

g) static fluid pressure plus gas overpressure to simulate the design loads during the hydrostatic testing of the tank,
h) self-weight loading associated with the tank lifting for final placement of the cargo tank in the ship.

4.2 Balsa/Polyurethane Foam Insulation and Secondary Barrier

As mentioned previously the cargo tank is supported on a series of plywood/balsa island panels arranged in longitudinal rows and around the periphery of the hold. These panels, Figure 7, are epoxy bonded around their periphery to timber grounds, which themselves are studded and bonded to the inner hull plate. A high strength epoxy matrix is used to fill the void between the bottom of the panel, timber grounds and inner hull.

As shown in Figure 8, the areas between the longitudinal rows of so-called island panels are filled with a polyurethane foam. These island panels and the polyurethane foam are the secondary barrier on the hull bottom.

Around the perimeter of each wall and bilge area a series of plywood/balsa panels is fitted to form picture frames for each side or bilge wall, Figures 7 and 8. Polyurethane foam is sprayed in layers, to a thickness of about 150 mm, to fill these balsa/plywood picture frames. This composite is the secondary barrier and insulation for these areas.

Additional insulation of the bottom and sides of the hold is obtained with 150 mm fibrous glass mats. The tank top insulation consists of 380 mm fibrous glass mats secured at their edges to the hold top edge panels.

When the cargo tank is filled the island panels compress more and the temperature gradient through these panels induces thermal stresses.

The fibreglass between the cargo tank and polyurethane foam keeps the top surface of the foam at about 194 K, i.e., approximately the temperature of solid carbon dioxide. The foam is stressed statically because of the temperature gradient through it and because of the still water bending of the hull.

At sea the wave motion on the hull [3, 11, 12] produces a variety of cyclic stresses in the secondary barrier. Hull bending produces a cyclic elongation and contraction of the secondary barrier. Ship roll produces a cyclic shear on the island panels supporting the tanks. Figure 9 shows the transverse pressure distribution within a tank for a typical ship motion. All of these must be studied to determine the compressive and shear loads acting on each island panel.

After discharging most of its cargo the ship returns with the tanks still at 111 K and with water in the ballast space. Depending upon the ship construction the ballast tanks may extend up to the deck overflow pipes and down to the inner hull bottom. During this ballast voyage the wave motions on the hull induce cyclic pressures in the ballast tanks. These static and cyclic ballast pressures are transmitted to the secondary barrier through the inner hull plating.

The effects of these various loadings on the secondary barrier have been investigated by finite element analyses and by static and fatigue testing. Some aspects of the fatigue tests will be discussed to illustrate the experimental design.

4.3 Ballast Pressure Fatigue Test

Figure 10 shows the detailed design of the fatigue panel and its relationship to one bay in the inner hull bottom. Figure 11 shows a general view of the test panel bolted and clamped to the base of the test rig. The inner hull plates and intermediate stiffeners, Figure 10, deflect under the action of the ballast pressure. Since the foam has a very low modulus compared to the steel hull the neutral axis for bending is near the centre of the inner hull plate. Therefore, there is a very significant magnification of strains at the top (cold) surface of the foam. Since the ballast pressure is cyclic it was necessary to calculate the ballast pressure spectrum and investigate its effect on the integrity of the secondary barrier.

The length of the test panel was determined by the spacing of the ship's longitudinal girders, since the island panels are installed in the line of the girders, Figures 5 and 10. The test panel is slightly longer than the spacing of the longitudinal girders to allow clamping of the balsa pads. These clamps, which have strain-gauged bolts, Figure 11, simulate the pressure of the tank and cargo acting on the balsa pads.

The width of the test panel was determined by the requirements that each balsa pad include a full-size plywood scab joint, Figure 7; that the inner hull plate and intermediate plate stiffeners be full-size, and that the central area of the test panel see full biaxial thermal restraint. A finite element analysis was used to investigate the effect of free edges on the thermal stresses in a slab of foam bonded to full thickness inner hull plate.

It was concluded that the test panel should be 2050 mm wide to correspond to the expected lines of inflexion of a bay in the inner hull bottom, Figure 10. To simulate these lines of inflexion (equivalent to simply supported edges) the side plates of the test panel were thin relative to the inner hull plate and the intermediate stiffeners were not tied directly into these side plates.

Before Kaiser Aluminum and Chemical Corporations foamed the first of these test panels it was strain-gauged, inside and outside, and fitted with deflection gauges so that the effect of internal pressure could be compared to the deflection patterns predicted by finite element and classical stress analyses. Estimated deflection patterns had been used previously as the input for a finite element analysis of the effect of ballast pressure on the foam.

The ballast pressure loads applied to these test panels were derived from acceleration spectra computed by Lloyds Register of Shipping, London, for a 130,000 m^3 LNG ship. These spectra were based on 20 years service in the North Atlantic with the ship sailing into a head sea and in ballast for 50% of its voyages. The ballast pressure fatigue spectrum shown schematically in Figure 12a was developed for a particular case; i.e., plating on the bottom edge of the forward transverse bulkhead of the forward hold of the three ships currently under construction at Avondale Shipyards.

It should be noted that the abcissa of Figure 12a shows the number of cycles exceeding a particular dynamic pressure p_i. This spectrum is converted into blocks of fatigue loading as shown in Figure 12a. It can be seen that there will be $n_1 - n_2$ cycles where the dynamic pressure is greater than p_1 and less than p_2. To be conservative one assumes that all of these cycles will occur at the higher pressure, i.e., p_2. This approach gives a block spectrum for 20 years of:

$n_1 - n_2$ cycles at $\pm p_2$ plus static ballast,

$n_2 - n_3$ cycles at $\pm p_3$ plus static ballast,

$n_3 - n_4$ cycles at $\pm p_4$ plus static ballast,

ending with

$n_i - n_{i+1}$ cycles at $\pm p_{i+1}$.

Obviously, the factor of safety on pressure depends on the choice of p_1, $p_2 \ldots$, p_{i+1}. The factor of safety on life can be obtained by either a simple extension of the pressure spectrum beyond twenty years or by operating with a variable factor on life. In either case, it is desirable to divide the twenty year block shown above into smaller blocks to reduce the uncertainties introduced by using an ordered rather than a real distribution of the pressures p_1, $p_2 \ldots p_{i+1}$ within the chosen cycle block. In most of these tests eleven levels of pressure were applied in each small block and it required two months to test to the equivalent of 40 years at sea.

Part of the pressure spectrum shown in Figure 12a was eliminated, i.e., pressures below $\pm p_1$. This was justified using the construction shown schematically in Figure 12b. This approach is an adaptation of one suggested some years ago for aircraft components [13]. The small specimen "Goodman" boundary, AB, was reduced on the ordinate to allow for the inevitable differences in fatigue strength between small specimens and large test panels. This so-called failure boundary, CA, was then reduced by a factor of three on the ordinate to give the operating boundary DA. The factor of three allows for scatter in fatigue strength and uncertainty in defining the stress distribution in the panel.

When defining the test spectrum, dynamic pressures which fell below the aforementioned operating boundary were eliminated. In most of these ballast pressure tests the dynamic pressures (stresses) not included in the fatigue spectrum were a factor of six below the estimated mean fatigue limit of small specimens.

The ballast pressure spectrum described above was applied with the sides of the test panel insulated and the top surface cooled with solid carbon dioxide. Test panels which had been fatigued in this manner for the equivalent of 40 years at sea or by applying cyclic bending [14] were also used to evaluate the response of the foam to an accident, i.e., leaking cargo tank, at some time during the service life. In these accident studies the top surface of the panel was cooled with liquid nitrogen in plastic bags on the foam surface (77 K) or in aluminum trays suspended above the foam surface (111 K). The panel was then subjected to cyclic loading. In some cases this cyclic loading corresponded to sailing the ship for a period of one month with cargo leaking from the aluminum tank onto the secondary barrier. The USCG requirements for certain types of primary barrier, given in the introduction of this paper, serve to explain why cyclic loading, equivalent to one month at sea, is a conservative approach to this problem.

4.4 Shear Fatigue of Model Island Panels

The object of these tests was to investigate the effect on island panels of cyclic shear due to ship roll. The interaction of the inner hull, island panels and cargo tank is such that the island panels will normally cycle

between shear deflection rather than load limits. If a panel cracks some load will be shed to adjacent panels and their shear deflection will increase slightly.

The compressive load and shear deflection of each island panel was obtained by finite element analysis of transverse sections of the tank and its supports with the tank subjected to pressure distributions similar to that shown in Figure 9.

Figure 13 shows the test rig designed to apply compression and cyclic shear to model island panels. These panels, K, were tested in pairs. Through the thickness these panels were full-size, which ensured that realistic (preferential) crushing occurred in tests where the panels were subjected to compressive overload.

To facilitate assembly, the wooden grounds and model panel are mounted on a sub-plate, A., using the mastic and adhesive discussed earlier. The sub-plate, A., bolts to the floating face-plate B of a pressure box, C. The two pressure boxes are connected by tie-rods, D, which pass through clearance holes in the sub-plates and model panels.

Hydraulic jacks on the four tie rods are connected to a common pressure source. If hydraulic pressure is applied to these jacks or directly inside the pressure boxes, C, the floating faceplates press the model panels against the sides of the cryogenic tank, E. The hollow cryogenic tank is machined from a solid slab of 5083-0 Al alloy and is fed from the top with a continuous supply of liquid nitrogen.

The cryogenic tank is connected through a clevis and strain-gauged load cell, F, to a servo-controlled hydraulic ram, G. This ram pushes and pulls the cryogenic tank to apply shear deflections to the model panels. The floating faceplates hang from the top crossbeam of the test rig. Backlash is minimized by tensioning the bolts, H, connecting the faceplates to the bottom crossbeam. Four spacer bars, J, were used to eliminate undesirable rotations of the faceplates.

The block loading spectrum for these tests was derived, using the procedure described in the previous section, from the roll spectrum for a 130,000 m^3 LNG tanker (supplied by Lloyds Register of Shipping, London) and finite element analyses of transverse sections of the containment system. All tests were run to at least the equivalent of 40 years of sailing in the North Atlantic.

This completes the discussion of some of the factors affecting the design and failure analysis of containment systems for the marine transportation of LNG. As with aircraft structures it is frequently necessary to test large sections of structure to obtain realistic load distributions (particularly thermal) and an appreciation of the possible modes of failure. A general statement of rules (existing and proposed) governing the design, construction and operation of self-propelled vessels carrying bulk liquified gases has recently been published by the U. S. Department of Transportation [15].

ACKNOWLEDGEMENTS

The authors wish to thank their co-workers who have contributed to the studies reported herein, G. Achenbach, W. L. Cuthbert, M. Goldberg, U. H. Mohaupt and A. H. Schwendtner. The authors thank Conch LNG for permission to publish this paper.

REFERENCES

1. CLARK, L. J., Proc. Inst. of Mechanical Engineers, London, 180, Part 1, 1965-1966.
2. THOMAS, W. du Barry and SCHWENDTNER, A., Proc. of Society of Naval Architects and Marine Engineers, New York, 1971.
3. BASS, R. L., HOKANSON, J. C. and COX, P. A., U. S. Coast Guard Ship Structure Committee Report SSC 258, 1976, 4-7.
4. JACKSON, R. G. and KOTCHARIAN, M., Proc. of First International Conf. on LNG, Chicago, 1968.
5. BURNS, D. J., JACKSON, R. G. and KALBFLEISCH, J. F., Proc. of Int. Conf. on Liquified Natural Gas, Int. Inst. of Refrigeration and Institution of Mechanical Engineers, London, 1969, 469-486.
6. TENGE, P., SOLLI, O. and FORLI, O., ASTM STP 579, 1975, 10-41.
7. ARGY, G., PARIS, P. C. and SHAW, F., ASTM STP 579, 1975, 96-131.
8. SAKAI T. et al, ASTM STP 579, 1975, 205-236.
9. KELSEY, R. A., WYGONIK, R. H. and TENGE, P., ASTM STP 579, 1975, 44-74.
10. GOLDBERG, M. and BROWN T., Cryogenic Society of America, Proc. of CRYO/75, Paper VI.
11. LEWIS, E. V. et al, U. S. Coast Guard Ship Structure Committee Report SSC 240, 1975.
12. HOFFMAN, D. et al, U. S. Coast Guard Ship Structure Committee Report, SSC 234, 1972.
13. DOUGHERTY, J. E. and SPICER, H. C., ASTM STP 338, 167.
14. POTTS, W. K. and CUTHBERT, W. L., Proc. Society of Naval Architects and Marine Engineers, New York, 1975.
15. Department of Transportation, U. S. A., Federal Register, 41, No. 193, October 4, 1976.

Table 1

Name	Methane Pioneer	Methane Princess	Gadania	El Paso Avondale
Length (m) (Overall)	103.2	189.3	259	284
Beam (m) (Molded)	15.2	24.8	35	42.8
Depth (m) (Molded)	12.5	17.8	n.a.	28.7
Draft (m)	7.2	7.9	9.5	11
Cargo Tank				
Design	Free Standing	" "	Conch Ocean	Free Standing
Type	Prismatic	" "	Membrane	Prismatic
Material	Aluminum	" "	Stainless Steel	Aluminum 5083
Capacity (m^3)	5123	27,400	75,000	125,000
Insulation	balsa	balsa	balsa	balsa/polyure-thane foam (PUF)
Secondary Barrier	plywood	plywood	plywood	plywood/PUF

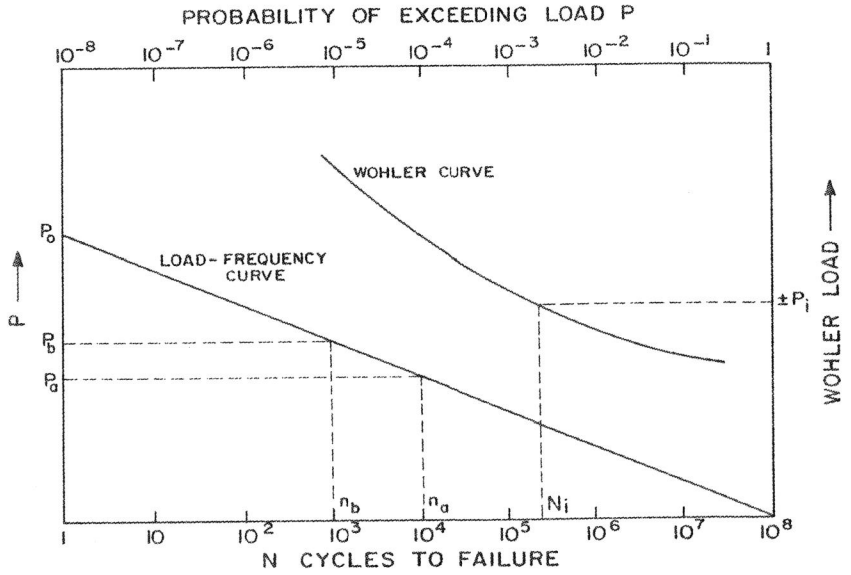

Figure 1 Load Spectrum and Wohler Curve

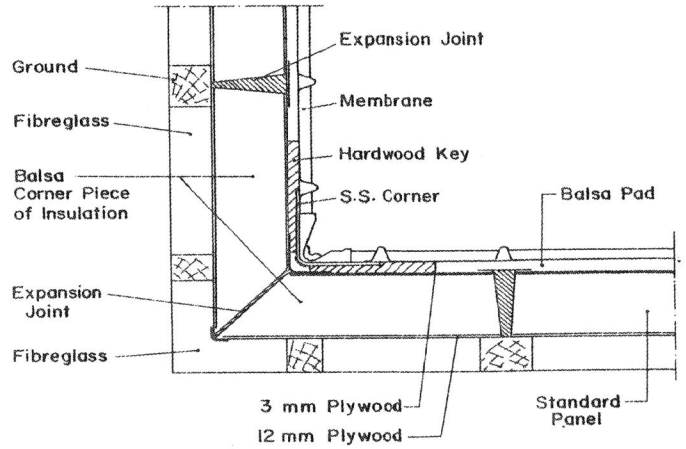

Figure 2 Conch Ocean Membrane System

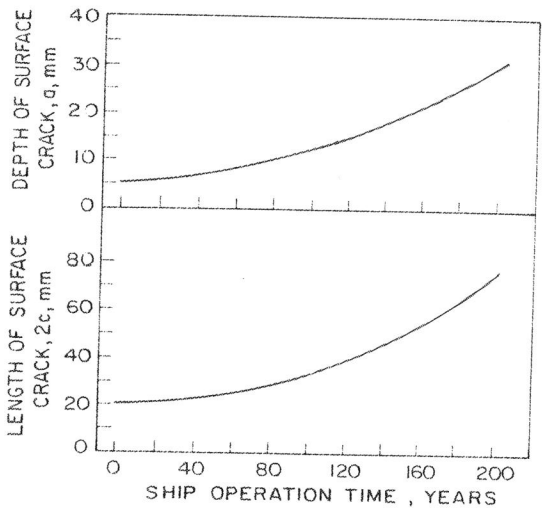

Figure 3 Surface Crack Growth in 5083-0 Al Alloy at 111°

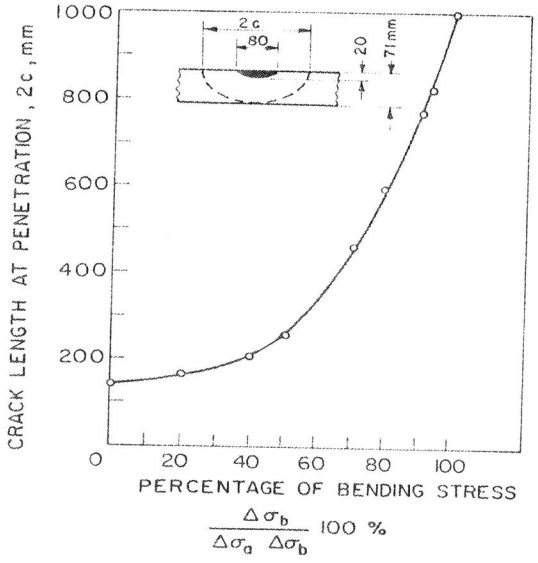

Figure 4 Surface Crack Length at Penetration for Axial Plus Bending Stress

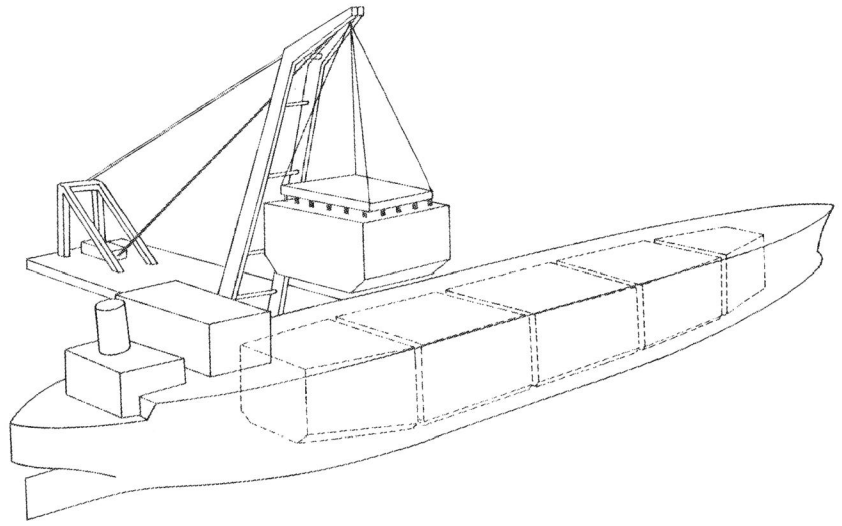

Figure 5 LNG Ship Designed for Self-Supporting Prismatic Tanks

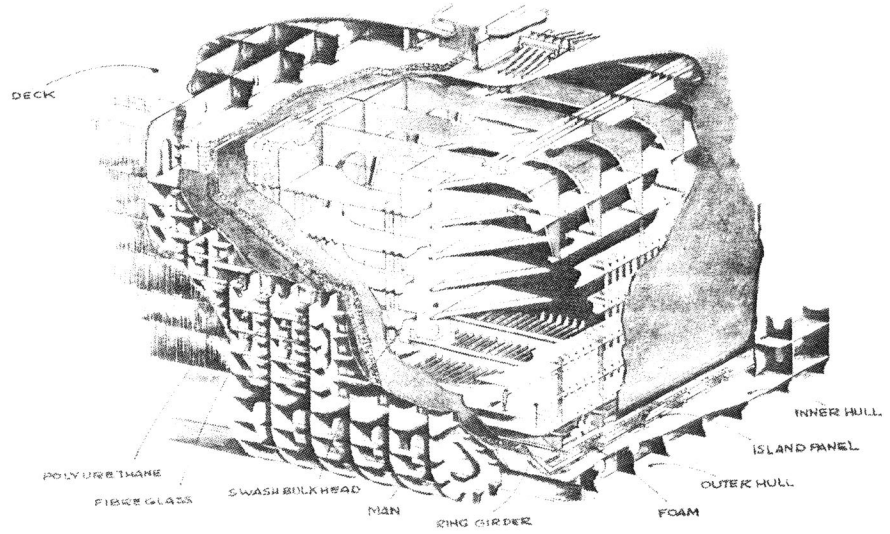

Figure 6 Conch Containment System Utilizing Self-Supporting Tanks

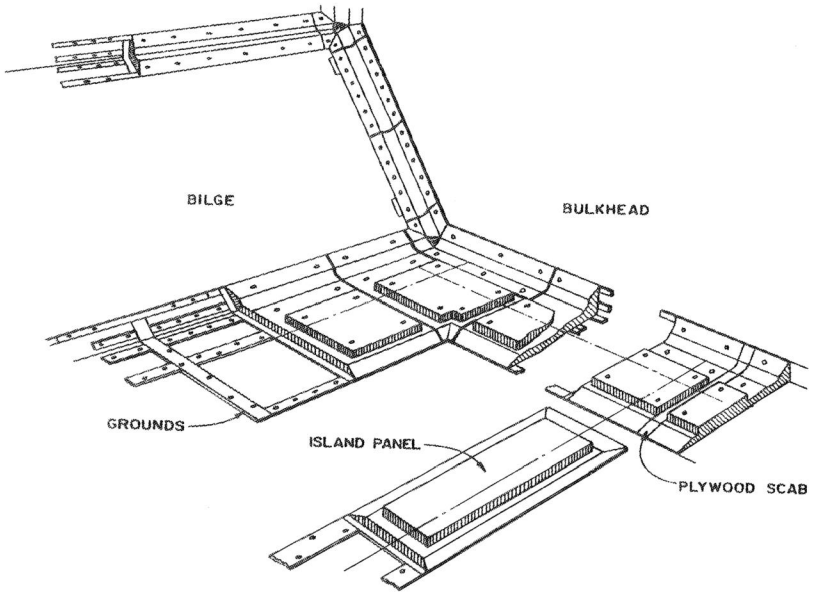

Figure 7 Balsa/Plywood Panels in Hold Corner

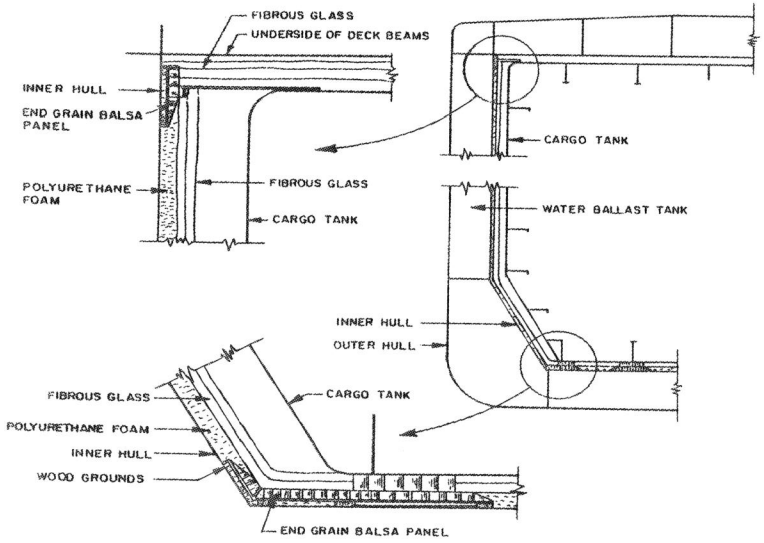

Figure 8 Transverse Section of Insulation and Secondary Barrier

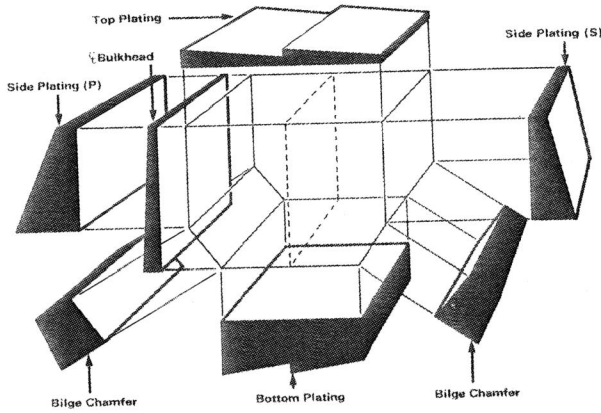

Figure 9 Transverse Pressure Distribution in Cargo Tank

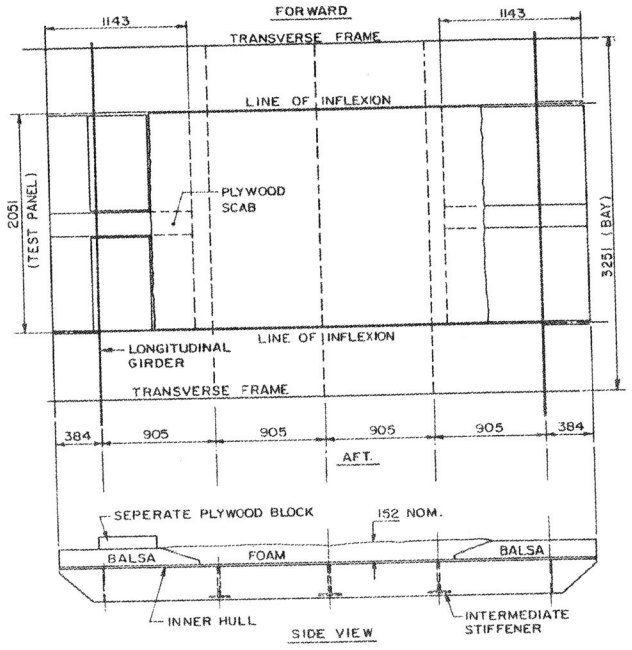

Figure 10 Relationship of Ballast Pressure Test Panel to Inner Hull Structure

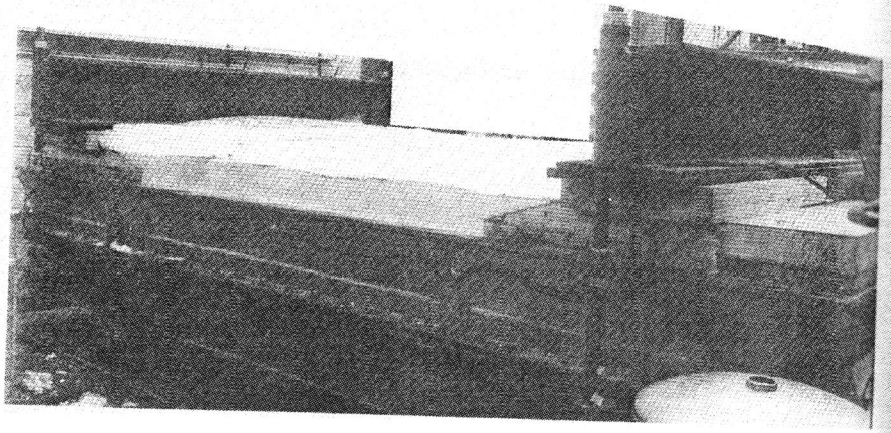

Figure 11 Ballast Pressure Test Rig

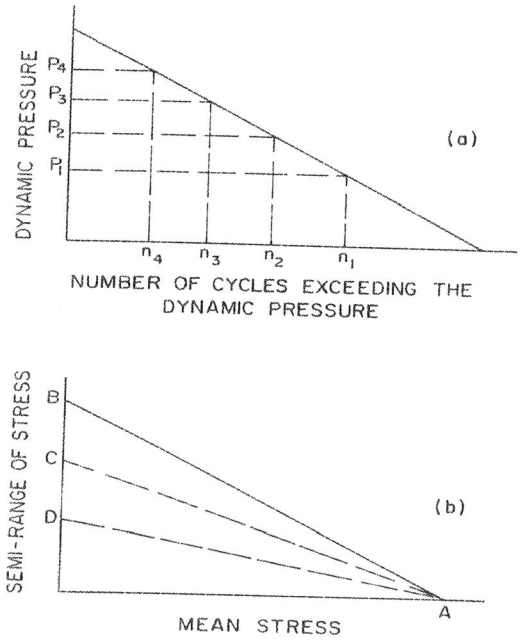

Figure 12 Load-Frequency and Fatigue Curves Used to Generate Block Loading Spectrum

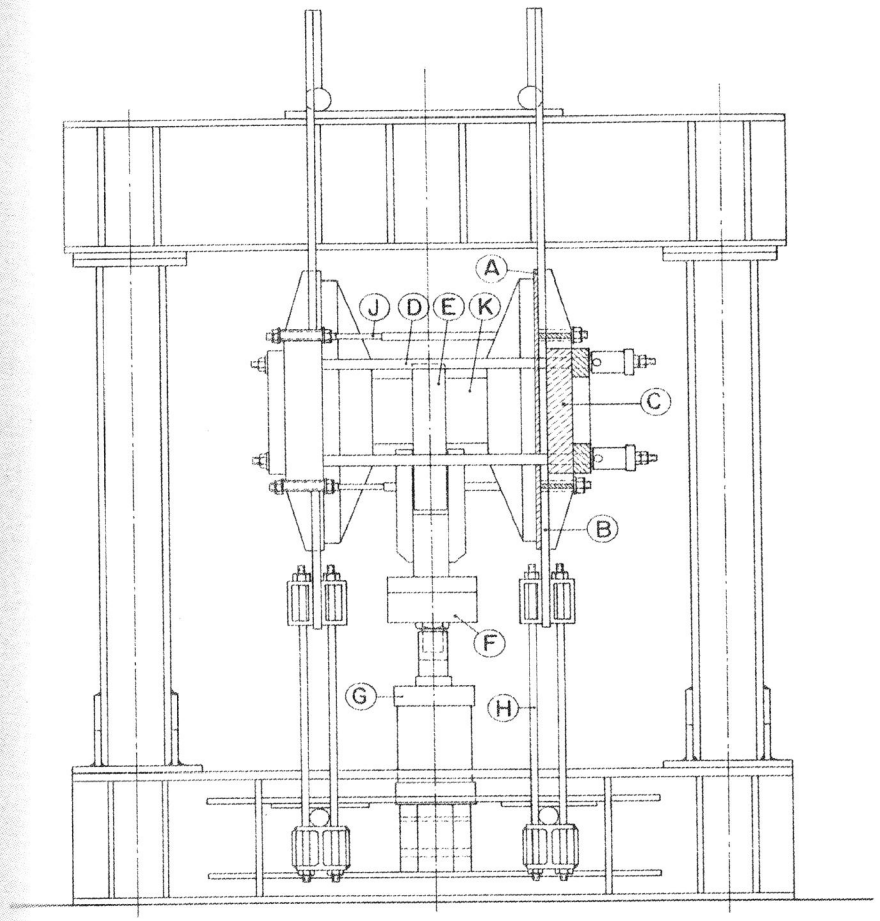

Figure 13 Rig for Compression and Cyclic Shear Tests on Model Island Panels